Asian Journal of Chemistry; Vol. 27, No. 6 (2015), 2231-2236

ASIAN JOURNAL OF CHEMISTRY

http://dx.doi.org/10.14233/ajchem.2015.18616

Preparation of C_{60} Nanowhiskers-ZrO_2 Nanocomposites and Kinetics for Photocatalytic Degradation of Organic Dyes

HAE SOO PARK and WEON BAE KO*

Department of Chemistry, Sahmyook University, Seoul 139-742, Republic of Korea

*Corresponding author: Fax: +82 2 9795318; Tel: +82 2 33991700; E-mail: kowb@syu.ac.kr, kowbsahmyook@syu.ac.kr

Received: 19 August 2014; *Accepted*: 28 November 2014; *Published online*: 17 March 2015; AJC-17000

C_{60} nanowhiskers were synthesized by liquid-liquid interfacial precipitation method and characterized by UV-vis, Raman spectrophotometer, X-ray diffraction (XRD), transmission electron microscopy (TEM) and scanning electron microscopy (SEM). Microwave irradiation was applied to prepare ZrO_2 nanoparticles using an aqueous solution of NH_4OH containing zirconyl chloride. ZrO_2 nanoparticles were confirmed by XRD, TEM and SEM. The C_{60} nanowhiskers-ZrO_2 nanocomposites were heated in an electric furnace at 700 °C under an inert Ar gas atmosphere for 2 h. The crystallinity, morphology and photocatalytic degradation activity of the C_{60} nanowhiskers-ZrO_2 nanocomposites were characterized by XRD, SEM, TEM, and UV-vis spectrophotometer. The ZrO_2 nanoparticles and C_{60} nanowhiskers-ZrO_2 nanocomposites were evaluated as a photocatalyst for the photocatalytic degradation of various organic dyes under ultraviolet light at 254 nm. We have discussed about kinetics of the photocatalytic degradation of methylene blue, methyl orange, rhodamine B, and brilliant green with the synthesized C_{60} nanowhiskers-ZrO_2 nanocomposites.

Keywords: C_{60} nanowhiskers, Zirconium dioxide nanoparticles, Photocatalytic degradation, Organic dyes.

INTRODUCTION

Fullerene (C_{60}) is received much attention in materials chemistry due to their extensive potential application[1]. Fullerene has been researched in optoelectrical devices, semiconductors, superconductors and composite materials[2,3]. Recently, various researches have been attempted for make nano sized carbon materials with many kinds of type such as fullerene, graphene, nanotubes and nanowhiskers[4-7]. Liquid-liquid interfacial precipitation (LLIP) method is proposed that the crystal formation mechanism is driven by supersaturation related to the limited bit solubility of C_{60} in alcohol[8]. LLIP method is simple and good method for synthesizing C_{60} nanowhiskers[9-11]. C_{60} nanowhiskers are expected to be important for potential applications in various fields, such as fuel cells, solar cells and catalysts[12].

Recently, nanomaterials as ZrO_2 and ZnO have attracted worldwide attention owing to their unique properties compared to those of their bulky counterparts[13]. Zirconium dioxide (ZrO_2) is considered one of the most important materials owing to its superplasticity, excellent ionic conductivity at high temperatures, high hardness and strength[14]. ZrO_2 is used in a range of industrial applications including optical waveguides, solid-state electrolytes, oxygen sensors and fuel cell membranes[15,16]. In particular, its photocatalytic properties has attracted considerable interest for applications in environmental purification and the decomposition of toxic and organic compounds[17].

The microwave-assisted hydrothermal technique is one of the desirable methods for nanoscale synthesis[18,19]. This is because microwave-assisted hydrothermal technique provides simple, fast and energy saving[20,21]. It is a clean method of synthesis and obtained fast with high purity and quite narrow size distribution of nanoparticles[22].

Wastewater containing organic dyes from textile, paper and some other industries are not readily decompose naturally[23]. Therefore, if these dyes are released into the environment, it is possible that the dyes destroy the ecosystems[24]. Metal oxide semiconductor materials, such as TiO_2, ZnO and ZrO_2 as photocatalysts have attracted a lot of attention due to the ability to degrade environmental pollutants under UV irradiation[25,26].

This paper reports the preparation of C_{60} nanowhiskers, heated ZrO_2 nanoparticles and C_{60} nanowhiskers-ZrO_2 nanocomposites. C_{60} nanowhiskers-ZrO_2 nanocomposites were heated to 700 °C in an electric furnace under an inert Ar gas atmosphere for 2 h[27,28]. The photocatalytic effects of the C_{60} nanowhiskers-ZrO_2 nanocomposites on the photocatalytic degradation of organic dyes were examined under ultraviolet light at 254 nm using a UV-visible spectrophotometer.

EXPERIMENTAL

Tetrahydrofuran (THF), isopropyl alcohol (IPA), benzene and ethanol were obtained from Samchun Chemicals. Zirconyl chloride octahydrate ($ZrOCl_2 \cdot 8H_2O$) and the organic dyes [methylene blue (MB), methyl orange (MO), rhodamine B (RhB) and brilliant green (BG)] were purchased from Sigma-Aldrich. C_{60} was supplied by Tokyo Chemical Industry Co., Ltd.

The samples were heat-treated in an electric furnace (Ajeon Heating Industry Co., Ltd). Microwave irradiation was performed in a domestic oven (2450 MHz, 700 W) at the maximum power in continuous heating mode. The crystal structure of the samples was investigated by X-ray diffraction (XRD, Bruker, D8 Advance) using CuK_α (λ = 1.5406 Å) radiation. The morphology and particle size of the samples were examined by transmission electron microscopy (TEM, JEOL Ltd., JEM-2010) at an acceleration voltage of 200 kV. The surface of the samples was observed by scanning electron microscopy (SEM, JEOL Ltd, JSM-6510) at acceleration voltages ranging from 0.5 to 30 kV. The UV-visible spectra of the samples were obtained using an UV-visible spectrophotometer (Shimazu, UV-1601 PC).The samples were also analyzed by Raman spectroscopy (Thermo Fisher Scientific, DXR Raman Microscope). An UV lamp (8 W, 254 nm, 77202 Marne La Valee-cedex 1 France) was used as the ultraviolet light irradiation source.

Preparation of C_{60} nanowhiskers: C_{60} powder (7 mg) was dissolved in 2 mL of benzene, ultrasonicated for 0.5 h and filtered to remove any undissolved solid state C_{60}. The resulting C_{60}-saturated benzene solution was poured into a 20 mL vial and 10 mL of isopropyl alcohol was added slowly to form a liquid-liquid interface. The solutions in the vial were then mixed manually and stored in a refrigerator at 5 °C.

Synthesis of ZrO_2 nanoparticles under microwave irradiation: 0.1 M solution of zirconyl chloride octahydrate in 100 mL of distilled water was prepared. The pH of the solution was adjusted to 9 with an aqueous NaOH solution. During stirring, the solution transformed to a gel. The sample in the gel state was heated by microwave radiation for 5 min and washed 5 times with ethanol and dried to obtain solid state product for overnight.Synthesized ZrO_2 nanoparticles were heated in an electric furnace at 700 °C in argon atmosphere for 2 h. Then, heated ZrO_2 nanoparticles were cooled to room temperature in argon atmosphere for 5 h.

Preparation of C_{60} nanowhiskers-ZrO_2 nanocomposites: To synthesize C_{60} nanowhiskers-ZrO_2 nano composites, 10 mg of synthesized C_{60} nanowhiskers and 10 mg of heated ZrO_2 nanoparticles were dissolved separately in 5 mL of tetrahydrofuran. The two solutions were then mixed and stirred vigorously for 0.5 h. The mixed solution was poured into a vessel and dried to vaporize the organic solvent for 1 h. The vessel was heated to 700 °C in an electric furnace under an Ar atmosphere for 2 h. The sample was cooled to room temperature under an Ar atmosphere for 5 h.

Evaluation of photocatalytic degradation of organic dyes with heated ZrO_2 nanoparticles and C_{60} nanowhiskers-ZrO_2 nanocomposites: The synthesized heated ZrO_2 nanoparticles and C_{60} nanowhiskers-ZrO_2 nanocomposites were used as photocatalysts for the degradation of organic dyes. The synthesized heated ZrO_2 nanoparticles (5 mg) and C_{60} nanowhiskers-ZrO_2 nanocomposites (5 mg) were placed separately in a vial containing 10 mL of an aqueous organic dyes solution. The vial was irradiated with 254 nm light using an UV-lamp. The level of organic dye degradation by photocatalysts was analyzed by UV-vis spectrophotometry.

Kinetics for photocatalytic degradation of various organic dyes: The photocatalytic degradation kinetics of various organic dyes such as methylene blue, methyl orange, rhodamine B and brilliant green have been modeled with the first-order reaction kinetics equation. Data for photocatalytic degradation kinetics of various organic dyes were evaluated directly from experimental values by the regression analysis of the linear curve using the software package Microsoft Excel (Version 2010).

RESULTS AND DISCUSSION

Fig. 1 shows the UV-visible spectra of the C_{60} nanowhiskers synthesized by the liquid-liquid interfacial precipitation (LLIP method and dispersed in toluene. The spectra revealed peaks at λ_{max} = 541, 597 and 620 nm. Fig. 2 shows Raman spectra of the C_{60} nanowhiskers. The Raman shifts of the C_{60} nanowhiskers were observed at 265, 491 and 1457 cm^{-1}, which were assigned to the H_g (1) squashing, A_g (1) breathing and A_g (2) pentagonal pinch modes of the C_{60} molecules, respectively[29].

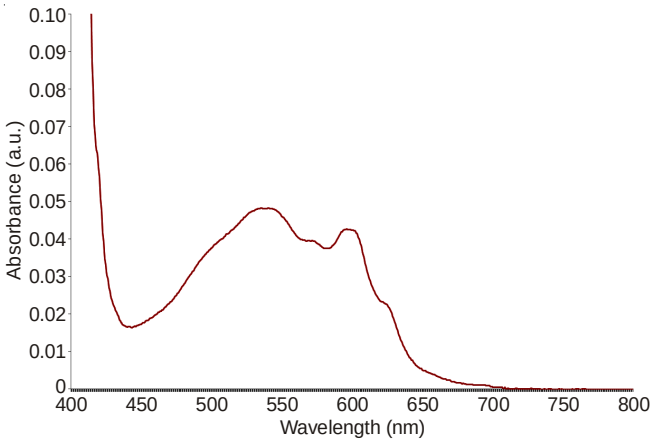

Fig. 1. UV-visibe spectrum of the synthesized C_{60} nanowhiskers

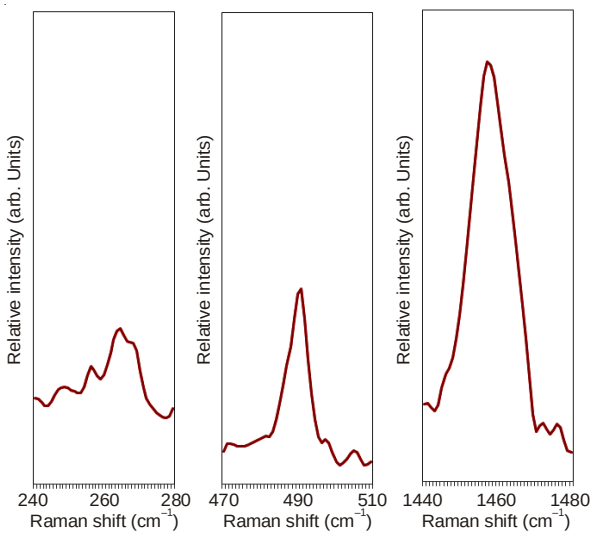

Fig. 2. Raman spectra of the synthesized C_{60} nanowhiskers

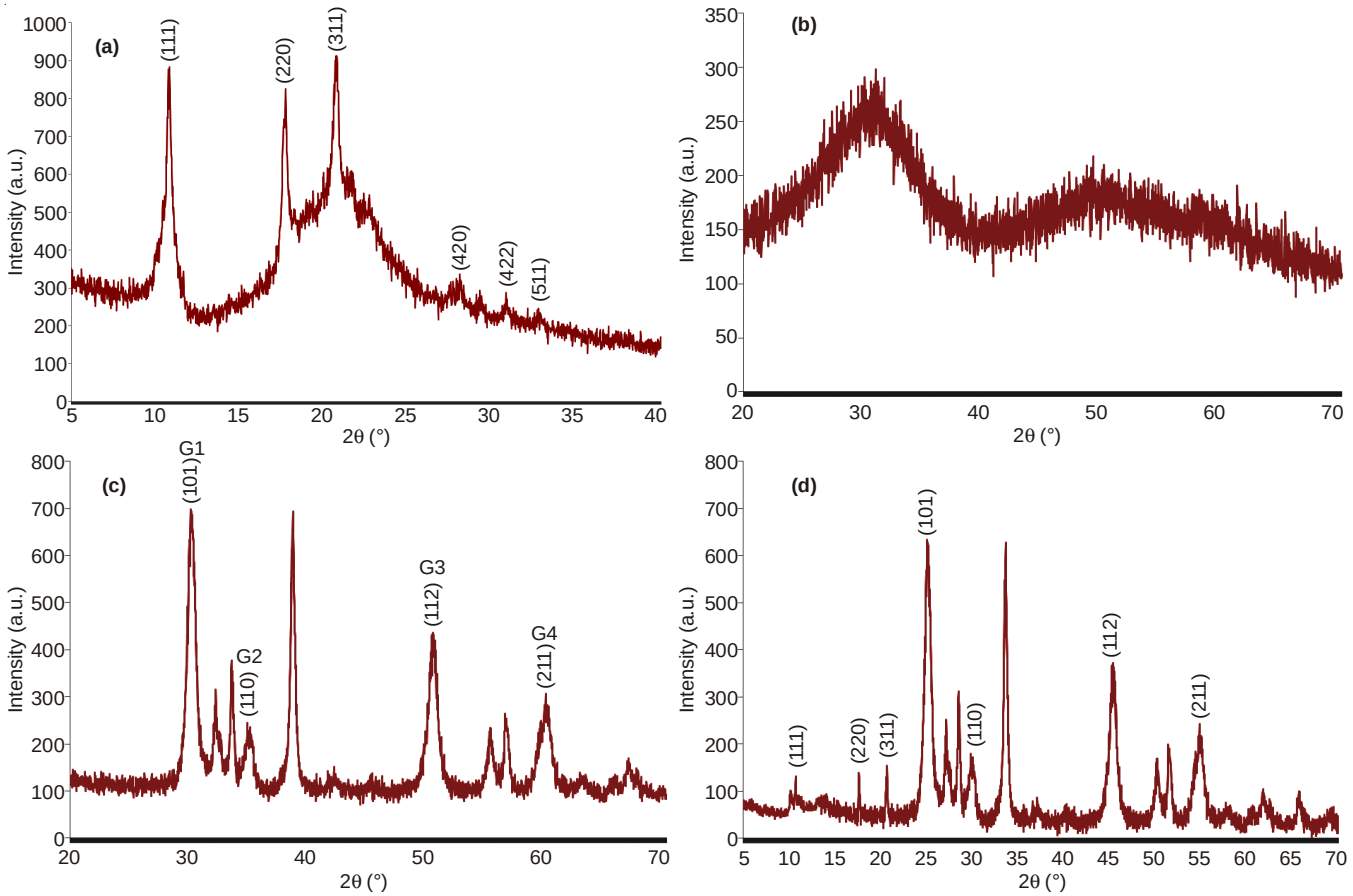

Fig. 3. XRD patterns of the (a) synthesized C_{60} nanowhiskers, (b) unheated ZrO_2 nanoparticles, (c) heated ZrO_2 nanoparticles and (d) C_{60} nanowhiskers-ZrO_2 nanocomposites

Fig. 3 shows XRD patterns of the (a) synthesized C_{60} nanowhiskers, (b) unheated ZrO_2 nanoparticles, (c) heated ZrO_2 nanoparticles and (d) C_{60} nanowhiskers-ZrO_2 nanocomposites. The characteristic peaks of the C_{60} nanowhiskers were observed at 10.80°, 17.70°, 20.74°, 28.08°, 30.82° and 32.75° 2θ, which were assigned to the [(111), (220), (311), (420), (422) and (511)] planes, respectively [Fig. 3 (a)]. The XRD pattern of the unheated ZrO_2 nanoparticles revealed an amorphous phase[30] [Fig. 3 (b)]. The characteristic peaks of the heated ZrO_2 nanoparticles were observed at 30.19°, 34.85°, 50.39° and 59.86° 2θ, which were assigned to the [(101), (110), (112) and (211)] planes, respectively [Fig. 3 (c)].

The crystallite size of the synthesized ZrO_2 nanoparticles was calculated using Scherrer's equation: $D = \frac{0.9\,\lambda}{\beta \cos\theta}$, where D is the crystallite size, λ is the wavelength of X-rays (0.15406 nm), β is the full width at half maximum (FWHM) of the diffraction peak and θ is the Bragg diffraction angle of the XRD peak in radians. Table-1 lists the mean crystallite size of the synthesized ZrO_2 nanoparticles; the mean crystallite size was 12.91 nm.

The characteristic peaks of the C_{60} nanowhiskers-ZrO_2 nanocomposites were observed at 30.19°, 34.85°, 50.39° and 59.86° 2θ due to ZrO_2 nanoparticles and 10.80°, 17.70°, 20.74°, 28.08°, 30.82° and 32.75° 2θ corresponding to C_{60} nanowhiskers [Fig. 3 (d)].

TABLE-1
MEAN CRYSTALLITE SIZE OF THE HEATED ZrO_2 NANOPARTICLES BY SCHERRER'S FORMULA

Peak	2θ	FWHM	D (nm)
G1	30.19	0.9059	18.17
G2	34.85	1.2997	12.81
G3	50.39	1.8616	9.43
G4	59.86	1.6346	11.22
Average			12.91

Fig. 4 shows TEM images of the (a) synthesized C_{60} nanowhiskers, (b) unheated ZrO_2 nanoparticles, (c) heated ZrO_2 nanoparticles and (d) C_{60} nanowhiskers-ZrO_2 nanocomposites. The synthesized C_{60} nanowhiskers had a rod and needle-like shape [Fig. 4 (a)]. The thickness of the C_{60} nanowhiskers ranged from 100 nm to 2 μm. The unheated ZrO_2 nanoparticles had a quasi-spherical and elliptical shape and were agglomerated [Fig. 4 (b)]. The mean size of the synthesized ZrO_2 nanoparticles was 20-70 nm. The heat treated ZrO_2 nanoparticles contained many pores [Fig. 4 (c)]. Because of this structure, the heated ZrO_2 nanocomposites had a large surface area. The C_{60} nanowhiskers were coated with ZrO_2 nanoparticles [Fig. 4 (d)]. The ZrO_2 nanoparticles were attached to the sides of the C_{60} nanowhiskers.

Fig. 5 shows SEM images of the (a) synthesized C_{60} nanowhiskers, (b) unheated ZrO_2 nanoparticles, (c) heated ZrO_2 nanoparticles and (d) C_{60} nanowhiskers-ZrO_2 nanocomposites. The synthesized C_{60} nanowhiskers showed a rectangular-rod

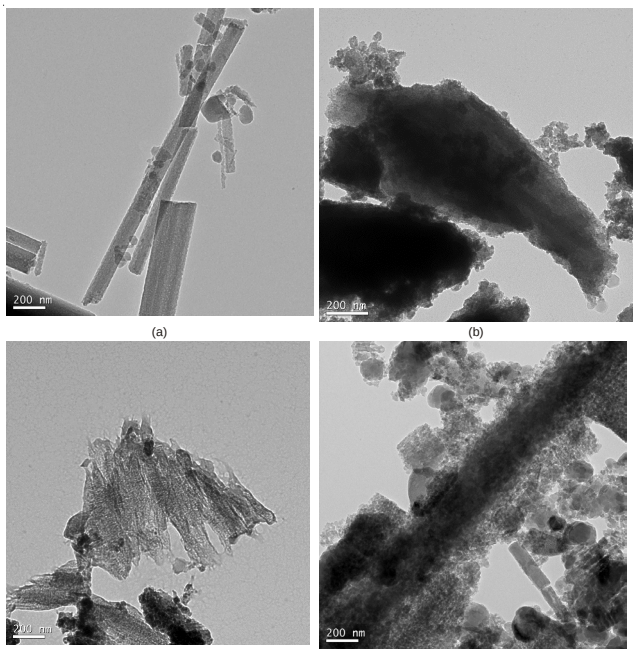

Fig. 4. TEM images of the (a) synthesized C_{60} nanowhiskers, (b) unheated ZrO_2 nanoparticles, (c) heated ZrO_2 nanoparticles and (d) C_{60} nanowhiskers-ZrO_2 nanocomposites

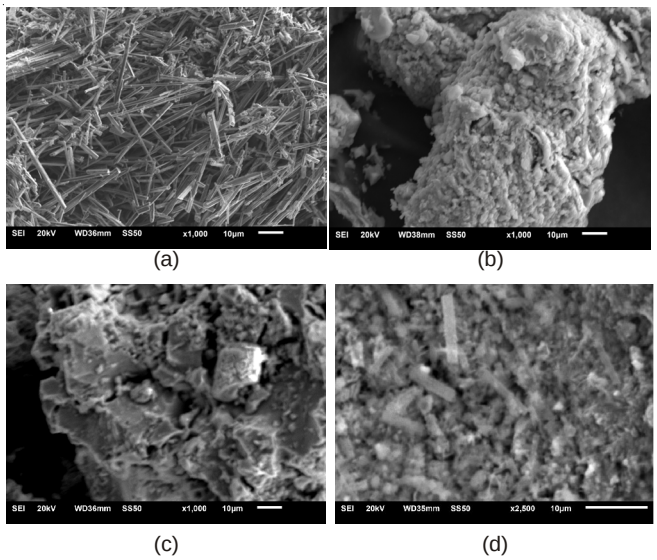

Fig. 5. SEM images of the (a) synthesized C_{60} nanowhiskers, (b) unheated ZrO_2 nanoparticles, (c) heated ZrO_2 nanoparticles and (d) C_{60} nanowhiskers-ZrO_2 nanocomposites

and needle-like morphology with fine agglomerates [Fig. 5 (a)]. The surface of the unheated ZrO_2 nanoparticles was wrinkled and agglomerated [Fig. 5 (b)]. The surface of the heated ZrO_2 nanoparticles had the appearance of rock like formations [Fig. 5 (c)]. C_{60} nanowhiskers were broken into smaller sizes [Fig. 5 (d)]. In addition, C_{60} nanowhiskers were attached to the surface of the ZrO_2 nanoparticles.

To confirm the photocatalytic performance, the degradation of organic dyes, such as methylene blue, methyl orange, rhodamine B and brilliant green, under UV irradiation at 254 nm for 5 min were examined by UV-visible spectrophotometry. Fig. 6 shows

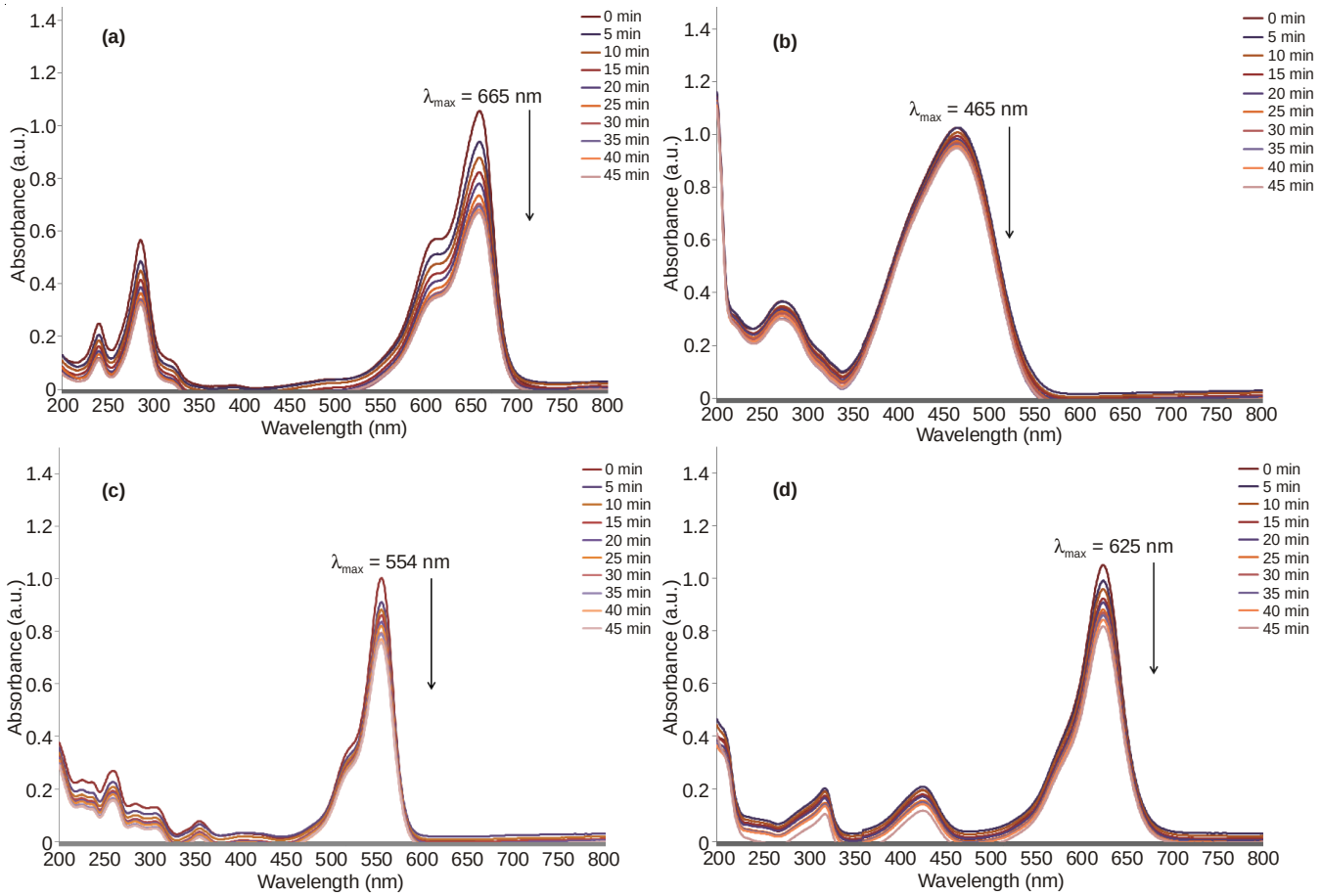

Fig. 6. UV-visible spectra of the degradation of (a) methylene blue, (b) methyl orange, (c) rhodamine B and (d) brilliant green with the heated ZrO_2 nanoparticles

the UV-visible spectra of the degradation of (a) methylene blue, (b) methyl orange, (c) rhodamine B and (d) brilliant green with the heated ZrO_2 nanoparticles under ultraviolet irradiation. The photocatalytic performance of the heated ZrO_2 nanoparticles was superior with methylene blue compared to rhodamine B, methyl orange and brilliant green. The degradation rates of rhodamine B and brilliant green were similar. The order of effectiveness among the organic dyes degraded was methylene blue > rhodamine B > brilliant green > methyl orange.

Fig. 7 shows UV-visible spectra of the degradation of (a) methylene blue, (b) methyl orange, (c) rhodamine B and (d) brilliant green using the synthesized C_{60} nanowhiskers-ZrO_2 nanocomposites under ultraviolet irradiation at 254 nm for 1 min. A comparison of Figs. 6 and 7 revealed the C_{60} nanowhiskers-ZrO_2 nanocomposites to be more efficient as a photocatalyst than the ZrO_2 nanoparticles alone. The C_{60} nanowhiskers had a significant effect on the photocatalytic degradation of the organic dyes. The addition of nano-carbon material to the matrix of suitable semiconductor materials (ZrO_2) can lead to a smaller band gap due to chemical bonding between the semiconductor nanoparticles and nano-carbon materials[31]. The order of effectiveness among the organic dyes degraded using C_{60} nanowhiskers-ZrO_2 nanocomposites as a photocatalyst was methylene blue > rhodamine B > brilliant green > methyl orange.

Fig. 8 presents the kinetics of the photocatalytic degradation of (a) methylene blue, (b) methyl orange, (c) rhodamine B and (d) brilliant green with the synthesized C_{60} nanowhiskers-ZrO_2 nanocomposites under ultraviolet irradiation at 254 nm for 1 min. The photocatalytic degradation of the various organic dyes followed first-order reaction kinetics according to

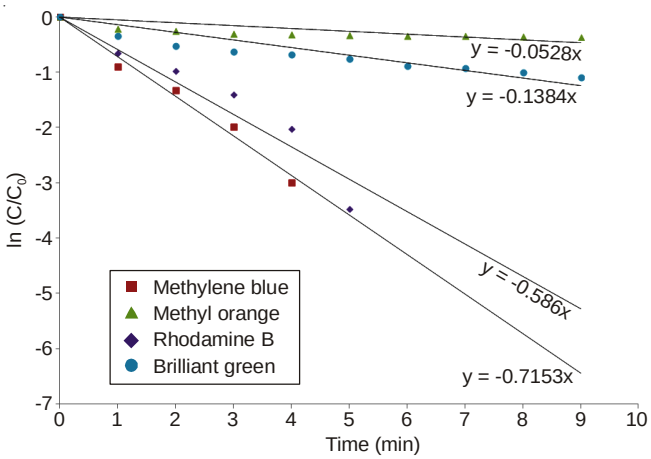

Fig. 8. Kinetics of the photocatalytic degradation of (a) methylene blue, (b) methyl orange, (c) rhodamine B and (d) brilliant green with the synthesized C_{60} nanowhiskers-ZrO_2 nanocomposites

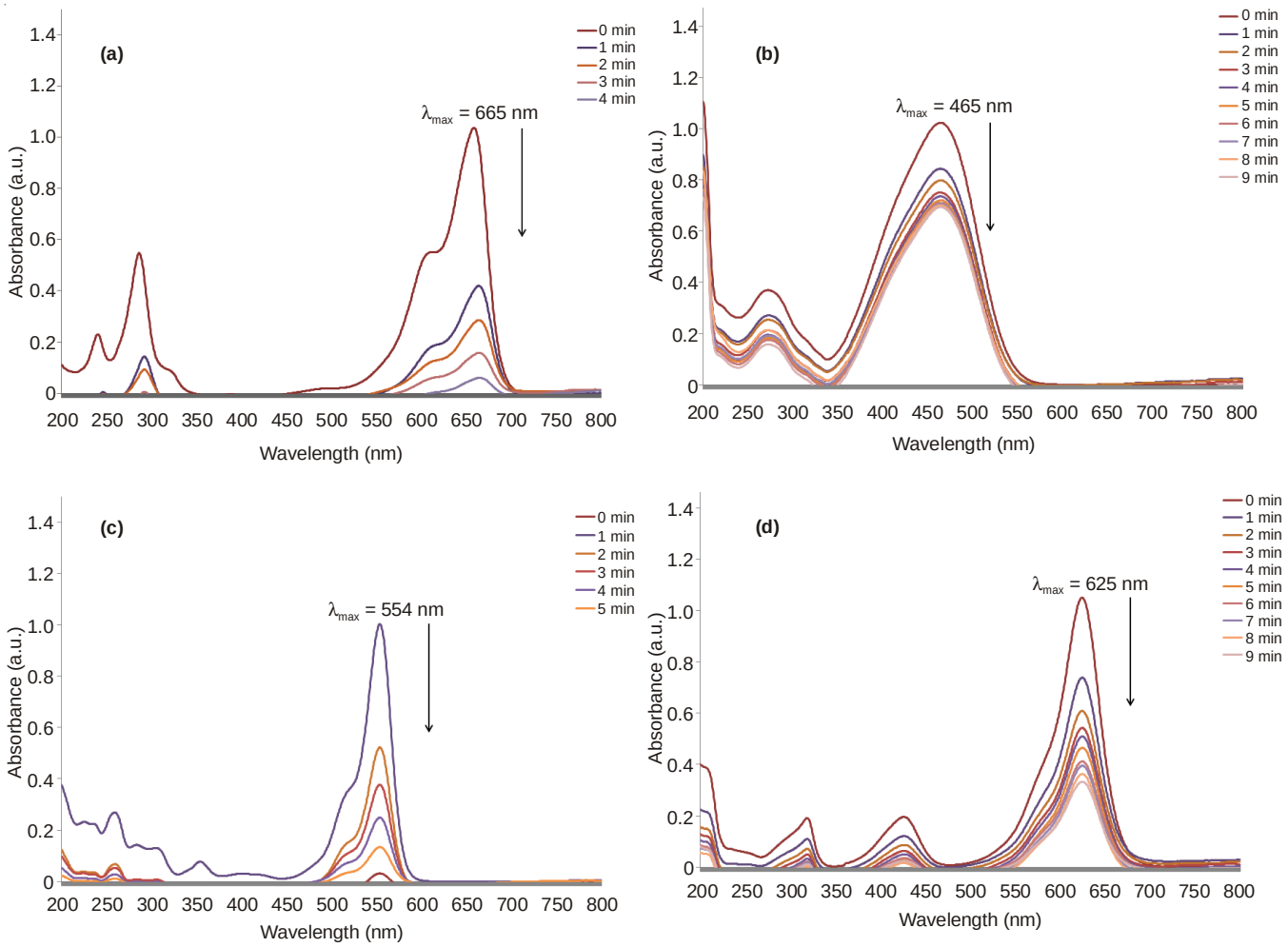

Fig. 7. UV-visible spectra of the degradation of (a) methylene blue, (b) methyl orange, (c) rhodamine B and (d) brilliant green with thesynthesized C_{60} nanowhiskers-ZrO_2 nanocomposites

TABLE-2
KINETICS OF THE PHOTOCATALYTIC DEGRADATION OF METHYLENE BLUE, METHYL ORANGE, RHODAMINE B AND BRILLIANT GREEN BY FIRST-ORDER REACTION WHICH IS KINETICS EQUATION

Time (min)	Methylene blue (ln C/C_0)	Methyl orange (ln C/C_0)	Rhodamine B (ln C/C_0)	Brilliant green (ln C/C_0)
0	0	0	0	0
1	-0.8950	-0.2076	-0.6478	-0.3445
2	-1.3246	-0.2515	-0.9795	-0.5293
3	-1.9827	-0.3003	-1.3996	-0.6296
4	-2.9920	-0.3139	-2.0265	-0.6842
5		-0.3266	-3.4641	-0.7580
6		-0.3381		-0.8795
7		-0.3453		-0.9236
8		-0.3531		-1.0062
9		-0.3627		-1.0933

the kinetics equation: $\ln\left(\frac{C}{C_0}\right) = -kt$, where C is the concentration according to the reaction time, C_0 is the initial concentration, k is the apparent first-order rate constant and t is the reaction time. Table-2 lists kinetics of the photocatalytic degradation of methylene blue, methyl orange, rhodamine B and brilliant green by first-order reaction which is kinetics equation. The order of the kinetics of the photocatalytic degradation of the organic dyes was methylene blue > rhodamine B > brilliant green > methyl orange (Table-2).

Conclusion

C_{60} nanowhiskers had a rectangular-rod and needle-like shape with sizes of 100 nm to 2 μm in width. After heat treatment, the ZrO_2 nanoparticles were porous with a large surface area. The mean crystallite size of the synthesized ZrO_2 nanoparticles was 12.91 nm according to Scherrer's equation. In C_{60} nanowhiskers-ZrO_2 nanocomposites, the C_{60} nanowhiskers were coated with ZrO_2 nanoparticles and ZrO_2 nanoparticles were attached to the sides of C_{60} nanowhiskers.The C_{60} nanowhiskers-ZrO_2 nanocomposites showed superior catalytic activity compared to ZrO_2 nanoparticles. The addition of C_{60} nanowhiskers promoted the photocatalytic degradation of organic dyes. Among the organic dyes (methylene blue, methyl orange, rhodamine B and brilliant green), methylene blue was decomposed the most effectively using the synthesized ZrO_2 nanoparticles and C_{60} nanowhiskers-ZrO_2 nanocomposites as a photocatalyst. The photocatalytic degradation of methylene blue, methyl orange, rhodamine B and brilliant green followed a first-order kinetics when C_{60} nanowhiskers-ZrO_2 nanocomposites were used as a photocatalyst. The reaction rate for the photocatalytic degradation of the organic dyes was in the order of methylene blue > rhodamine B > brilliant green > methyl orange.

ACKNOWLEDGEMENTS

This study was supported by Sahmyook University funding in Korea.

REFERENCES

1. M. Sathish and K. Miyazawa, *J. Am. Chem. Soc.*, **129**, 13816 (2007).
2. E.Y. Zhang and C.R. Wang, *Curr. Opin. Colloid Interface Sci.*, **14**, 148 (2009).
3. L.K. Shrestha, Y. Yamauchi, J.P. Hill, K. Miyazawa and K. Ariga, *J. Am. Chem. Soc.*, **135**, 586 (2013).
4. K. Miyazawa, *J. Nanosci. Nanotechnol.*, **9**, 41 (2009).
5. K. Miyazawa, Y. Kuwasaki, A. Obayashi and M. Kuwabara, *J. Mater. Res.*, **17**, 83 (2002).
6. L. Wang, B. Liu, D. Liu, M. Yao, Y. Hou, S. Yu, T. Cui, D. Li, G. Zou, A. Iwasiewicz and B. Sundqvist, *Adv. Mater.*, **18**, 1883 (2006).
7. Y. Jin, R.J. Curry, J. Sloan, R.A. Hatton, L.C. Chong, N. Blanchard, V. Stolojan, H.W. Kroto and S.R.P. Silva, *J. Mater. Chem.*, **16**, 3715 (2006).
8. L.K. Shrestha, J.P. Hill, T. Tsuruoka, K. Miyazawa and K. Ariga, *Langmuir*, **29**, 7195 (2013).
9. M. Sathish, K. Miyazawa and T. Sasaki, *Chem. Mater.*, **19**, 2398 (2007).
10. M. Sathish, K. Miyazawa, J.P. Hill and K. Ariga, *J. Am. Chem. Soc.*, **131**, 6372 (2009).
11. M. Sathish and K. Miyazawa, *J. Am. Chem. Soc.*, **129**, 13816 (2007).
12. K. Miyazawa and K. Hotta, *J. Cryst. Growth*, **312**, 2764 (2010).
13. N.C.S. Selva, A. Manikandan, L.J. Kennedy and J.J. Vijaya, *J. Colloid Interface Sci.*, **389**, 91 (2013).
14. M.J. Mayo, *Int. Mater. Rev.*, **41**, 85 (1996).
15. M. Zevin and R. Reisfeld, *Opt. Mater.*, **8**, 37 (1997).
16. A. Evans, A.B. Hûtter, J. L. Rupp and L. J. Gauckler, *J. Power Sources*, **194**, 119 (2009).
17. A.A. Ashkarran, S.A.A. Afshar, S.M. Aghigh and M. Kavianipour, *Polyhedron*, **29**, 1370 (2010).
18. M.N. Nadagouda, T.F. Speth and R.S. Varma, *Acc. Chem. Res.*, **44**, 469 (2011).
19. D. Synnott, M. Seery, S. Hinder, J. Colreavy and S. Pillai, *Nanotechnology*, **24**, 045704 (2013).
20. W.T. Yao, S.H. Yu, L. Pan, J. Li, Q.S. Wu, L. Zhang and J. Jiang, *Small*, **1**, 320 (2005).
21. E.C. Linganiso, S.D. Mhlanga, N.J. Coville and B.W. Mwakikunga, *J. Alloys Comp.*, **552**, 345 (2013).
22. N. Soltani, E. Saion, M.Z. Hussein, M. Erfani, A. Abedini, G. Bahmanrokh, M. Navasery and P. Vaziri, *Int. J. Mol. Sci.*, **13**, 12242 (2012).
23. M.A. Behnajady, N. Modirshahla and R. Hamzavi, *J. Hazard. Mater.*, **133**, 226 (2006).
24. Y.M. Slokar and A.M. Le Marechal, *Dyes Pigment.*, **37**, 335 (1998).
25. S. Danwittayakul, M. Jaisai and J. Dutta, *Appl. Catal. B*, **163**, 1 (2015).
26. R. Saleh and N.F. Djaja, *Superlattices Microstruct.*, **74**, 217 (2014).
27. S.K. Hong, J.H. Lee and W.B. Ko, *J. Nanosci. Nanotechnol.*, **11**, 6049 (2011).
28. B.H. Cho, S.W. Ko, W.C. Oh and W.B. Ko, *Asian J. Chem.*, **25**, 5063 (2013).
29. K. Miyazawa, Fullerene nanowhiskers, Pan Stanford Publishing Pvt. Ltd., Singapore, pp. 33-35 (2012).
30. B.H. Cho and W.B. Ko, *J. Nanosci. Nanotechnol.*, **13**, 7625 (2013).
31. K. Ullah, S. Ye, S. Sarkar, L. Zhu, Z.D. Meng and W.C. Oh, *Asian J. Chem.*, **26**, 145 (2014).